

Received Date : 30-Jan-2013
Revised Date : 22-Apr-2013
Accepted Date : 09-May-2013
Article type : Resource

Whole Genome Profiling Physical Map and Ancestral Annotation of Tobacco Hicks Broadleaf

Nicolas Sierro^a, Jan van Oeveren^b, Michiel J.T. van Eijk^b, Florian Martin^a, Keith E. Stormo^c,
Manuel C. Peitsch^a, and Nikolai V. Ivanov^{a,1}

^a Biological System Research, Philip Morris International R&D, Philip Morris Products S.A.,
Neuchatel, Switzerland

^b Keygene N.V., Agro Business Park 90, 6708 PW, Wageningen, The Netherlands

^c Amplicon Express Inc., 2345 NE Hopkins Ct., Pullman, WA 99163, USA

¹Corresponding author: Nikolai V. Ivanov, Biological System Research, Philip Morris
International R&D, Philip Morris Products S.A., Neuchatel, Switzerland. Tel. +41 (58) 242
2651. Fax +41 (58) 242 2811. E-mail: Nikolai.Ivanov@pmi.com

NS: Nicolas.Sierro@pmi.com

JvO: jan.van-oeveren@keygene.com

MvE: michiel.van-eijk@keygene.com

FM: Florian.Martin@pmi.com

This article has been accepted for publication and undergone full peer review but has not
been through the copyediting, typesetting, pagination and proofreading process which may
lead to differences between this version and the Version of Record. Please cite this article as
an 'Accepted Article', doi: 10.1111/tpj.12247

This article is protected by copyright. All rights reserved.

KES: keith@ampliconexpress.com

MCP: Manuel.Peitsch@pmi.com

NVI: Nikolai.Ivanov@pmi.com

Running title: WGP Physical Map of Tobacco Genome

Keywords: physical map, genome, tobacco, *Nicotiana tabacum*, ERP001765, polyploidy, Whole Genome Profiling, next generation sequencing

Summary

Genomics-based breeding of economically important crops such as banana, coffee, cotton, potato, tobacco and wheat is often hampered by genome size, polyploidy and high repeat content. We adapted the sequence-based Whole Genome Profiling (WGP™) technology to gain insight into the polyploidy of the model plant *Nicotiana tabacum* (tobacco). *N. tabacum* is assumed to originate from a hybridization event between *Nicotiana sylvestris* and *Nicotiana tomentosiformis* about 200,000 years ago. This resulted in tobacco having a haploid genome size of 4,500 million base pairs, about four times larger than the related tomato and potato genomes. In this study a physical map containing 9,750 contigs of bacterial artificial chromosomes (BACs) was constructed. The average contig size was 462 kbp, and the calculated genome coverage equaled the estimated tobacco genome size. We used a method for determination of the ancestral origin of the genome by annotation of WGP sequence tags. This assignment agreed with the ancestral annotation available from the tobacco genetic map and may be used to investigate the evolution of homoeologous genome segments after polyploidization. The map generated will be an essential scaffold for the tobacco genome. We propose the combination of WGP physical mapping technology with

Accepted Article

tag profiling of ancestral lines as a generally applicable method to elucidate the ancestral origin of genome segments of polyploid species. The physical mapping of genes and their origins will enable application of biotechnology to polyploid plants aimed at accelerating and increasing the precision of breeding for abiotic and biotic stress resistance.

Introduction

Tobacco (*Nicotiana tabacum*) is an allotetraploid species ($2n=4x=48$) and a member of the Solanaceae family, which includes eggplant, pepper, petunia, potato and tomato. A tetraploidization event, which occurred about 200,000 years ago (Leitch *et al.* 2008) and involved ancestors of *Nicotiana sylvestris* (S genome; $2n=24$) and *Nicotiana tomentosiformis* (T genome; $2n=24$) is likely to be responsible for its emergence (Lim *et al.* 2004, Clarkson *et al.* 2005). *N. tabacum* therefore has a relatively large genome size (approximately 4,500 Mb) compared with other cultivated Solanaceae crops (Arumuganathan *et al.* 1994), which is 50% larger than the human genome.

Analysis of the tobacco genome has been ongoing in the last decade. In 2001, the Tobacco Genome Initiative (TGI) was established to sequence the tobacco genome using the methyl-filtration method for genome complexity reduction (Rabinowicz *et al.* 1999). The Hicks Broadleaf variety, a breeding background of some flue-cured tobacco cultivars in use today, was chosen as the genotype for generation of the bacterial artificial chromosome (BAC) libraries used for sequencing because of its low introgression content. A total of 1,420,169 unique raw Sanger sequences with an average length of 697 bp were obtained and publicly released (Opperman, <http://www.pngg.org/tgi/index.html>). Although the genome assembly of these sequences by SOL Genomics Network (SGN, <http://solgenomics.net/>) is very informative, it remains highly fragmented. Its applicability is thus significantly reduced and a higher-quality draft genome of tobacco is still required.

A high-density tobacco map was built recently by applying simple sequence repeat (SSR) markers generated from the TGI to an F₂ mapping population derived from crossing *N. tabacum* Hicks Broadleaf and Red Russian varieties (Bindler *et al.* 2011). This genetic map is comparable in marker density and resolution with the latest tomato and potato genetic maps, and is likewise available from the SGN clade-oriented database containing genomic, genetic, phenotypic and taxonomic information for plants of the Solanaceae and Rubiaceae (coffee) families (Bombarely *et al.* 2011).

Advancements in modern breeding approaches of many economically important crops such as banana, coffee, cotton, potato, tobacco and wheat are hampered by genome size, polyploidy and high repeat content. Despite the progress in sequencing technologies achieved in the last decade, assembly of reference polyploid genomes is still challenging. One of the key enablers to achieve this goal is the construction of a high-quality physical map (Ariyadasa and Stein 2012). Recent examples of this approach include cotton and potato. Similar to tobacco, cultivated tetraploid cotton, *Gossypium hirsutum*, arose from combination of the A and D genomes about 1–2 million years ago. The whole physical map of *G. hirsutum* has been built using transformation-competent binary BACs and applying the High Information Content Fingerprinting (HICF) method using SNaPshot[®] (Zhang *et al.* 2012). A physical map of a related cotton species, *Gossypium raimondii*, whose progenitor is the putative contributor of the D genome to cultivated cotton, also has been constructed recently using the HICF method (Lin *et al.* 2010). The *Gossypium* physical maps serve as frameworks for anchoring and ordering the assembled sequences into the reference allotetraploid cotton genome.

Although a reference genome is available for the double-monoploid DM1-3 516 R44 potato (Xu *et al.* 2011), the Potato Genome Sequencing Consortium recognized the necessity to first build a physical map of a heterozygous diploid RH89-039-16 potato, using KeyGene's Whole Genome Profiling (WGP™) technology (de Boer *et al.* 2011), before embarking on the assembly of a reference genome for the cultivated tetraploid potato. For the large diploid genome of maize, the construction of a physical map was instrumental in generating chromosome-based pseudomolecules, leading to a first version of the maize B73 reference genome (Wei *et al.* 2009).

To further increase the quality of currently available tobacco resources to a par with those of tomato and potato, we constructed a physical map of tobacco using WGP technology. The constructed physical map is based on sequenced tags of the terminal ends of restriction fragments from pooled BAC clones produced using Illumina's Genome Analyzer II platform and assembled by an adapted FPC program (Soderlund *et al.* 1997, van Oeveren *et al.* 2011). The WGP method significantly differs from the competing SNaPshot® HICF technology (Ding *et al.* 2001, Luo *et al.* 2003, Luo *et al.* 2010) and can deliver a physical map of higher quality and wider utility because of the characteristics and quality of the sequence tags used for physical map assembly (van Oeveren, *et al.* 2011). The sequence-based nature of the WGP physical map of tobacco allowed us to determine the ancestral origin of a majority of the tobacco BACs and WGP physical map contigs by comparison to sequence tags obtained from *N. sylvestris* and *N. tomentosiformis*. In addition, we determined the origin of chromosomal regions by linking them to the available tobacco genetic map. Finally, we illustrate the usefulness of the WGP physical map to scaffold DNA sequences by integrating DNA sequences resulting from the SGN assembly of the TGI sequence data.

Results

WGP tags generation. A total of 1,107 384-well plates from four libraries (425,088 BAC clones) was subjected to WGP, as described by van Oeveren and co-workers (van Oeveren, *et al.* 2011). BAC pooling was performed in a two-dimensional format with each pool consisting of 48 clones. DNA isolated from these pools was digested with *EcoRI* and *MseI*, barcoded adapters were ligated, and restriction fragments were amplified. Amplicons were subsequently sequenced from the *EcoRI* restriction-site end using the Illumina Genome Analyzer II (GAII). In total this yielded 1,718 million reads with 78 nt read length with a valid sample identification tag and a proper restriction-site sequence. Deconvolution was carried out using the first 31 nt, the first 51 nt and the full 70 nt reads (excluding the barcode sequences), resulting in half of the total number of reads being assigned as WGP tags to individual BACs. After filtering these WGP tags on several quality criteria, a total of 1.2 million different WGP tags were mapped to 361,034 BACs for the 51 nt set (Table 1). Results for all three sets are presented in Table S1. The 51 nt WGP tag analysis was selected as the final data set because the analysis demonstrated that this read length provided a maximum number of deconvoluted reads.

Physical map construction. After conversion of the WGP tag data to pseudo-mobility numbers, the FPC software (Soderlund, *et al.* 1997) adapted for use with sequence tags as described in (van Oeveren, *et al.* 2011) was used to assemble sequence-based physical BAC maps. A cut-off value of 10^{-25} was used with a subsequent DQ-step to produce a high stringency map. Additional end-to-end contig and singleton merging steps at 10^{-15} were performed to obtain a normal stringency map with fewer contigs. Using the 51 nt set and normal stringency settings, the tobacco physical map comprised 9,750 contigs containing 330,632 BACs (77.8% of the BACs tested; 91.5% of the tagged BACs). Of the remaining

BACs, 30,402 did not link to any other BAC and were classified as singletons, and 64,064 BACs had no deconvoluted tags. The estimated average and N_{50} contig size were 462 and 689 kbp, respectively, and the calculated genome coverage was 4,508 Mbp (Table 1). Results of both stringency settings for all three sets are presented in Table S2.

Ancestral origin of tobacco BACs and WGP contigs. *EcoRI* restriction-site-flanking sequence tags for the whole genomes of *N. sylvestris* and *N. tomentosiformis*, the two closest relatives to the ancestral contributors of the S and T genomes to tobacco, were obtained by digesting genomic DNA of these lines with *EcoRI* and *MseI*, followed by amplification and *GAI* sequencing using the same method as applied for WGP map construction of *N. tabacum*. After quality filtering, 1,089,317 *N. sylvestris* and 1,035,343 *N. tomentosiformis* tags were compared with the 1,239,733 unique 51 nt tags obtained for *N. tabacum* during the construction of the physical map, thus allowing the determination of the ancestral origin of the tobacco tags, BACs and WGP physical map contigs by S or T tag enrichment *P*-value calculations. This analysis showed that 60.7% of the BACs are of S origin and 37.4% of T origin. The origin of 0.4% of the BACs could not be determined despite their S and/or T tags, and these BACs were classified as having an undefined origin. Finally, 1.5% of the BACs have no S or T tags and are thus of unknown origin. BACs consist of tobacco DNA fragments of about 100 kb, and as such should originate from only one of the two ancestors. Being able to assign an ancestral origin to 98.1% of the BACs indicates that S and T tags are not present randomly in BACs, and thus validates the origin determination of WGP tags. The S or T tag enrichment *P*-value calculations further showed that 53.7% of the WGP contigs are of S origin, 45.8% of T origin, 0.5% of undefined origin, and only four of unknown origin (Table 2, Figure 1). Thus the S and T tags are rarely found together in the same WGP contig, providing additional confidence in the quality of the constructed physical map.

Comparing the ancestral origin of BACs to the ancestral origin of the WGP contigs in which they were placed showed that the majority of the BACs of S or T origin were found in WGP contigs with the same origin annotation (98.0% and 94.0% for BACs of S or T origin, respectively) (Table 3). BACs of undefined origin were almost evenly placed in WGP contigs of S or T origin (43.8% and 53.1%, respectively), whereas 78.1% of the BACs of unknown origin were placed in WGP contigs of T origin and 19.4% in WGP contigs of S origin.

Taking advantage of the ordering of the BACs in a WGP contig (where no ordering is available for the tags in a BAC) and to complement the enrichment *P*-values, the number of domains composed of BACs of S or T origins was estimated for each WGP contig, as described in the Materials and Methods section. WGP contigs with a clear origin should ideally be composed of only one domain, whereas WGP contigs of undefined origin either possess more than one domain or are artifacts created during the WGP physical map construction. The number of domains counted in WGP contigs of S, T or undefined origin showed that only one domain was identified for 94.1% and 93.2% of the WGP contigs of S or T origins, respectively (Table S3). Enrichment *P*-values, which are only based on counts and do not consider contig units, are therefore well complemented by the domain structure, as some S (respectively T) contigs can contain several domains, with the majority corresponding to the assigned origin.

Linking the genetic and physical maps. The *N. tabacum* genetic map was constructed from a Hicks Broadleaf × Red Russian F₂ mapping population (Bindler, *et al.* 2011). It consisted of 24 linkage groups comprising 1,776 unique loci determined by 2,318 SSR markers. SSR amplification tests on *N. sylvestris* and *N. tomentosiformis* were then used to annotate tobacco linkage group regions according to their putative S or T ancestral origin. Of the 2,318 SSR

markers of the *N. tabacum* genetic map, 918 were experimentally linked to 910 BACs. In the WGP physical map, 802 of these BACs were contained in 725 WGP contigs.

The number of BACs and WGP contigs of S, T or undefined origin mapped to these S or T linkage group regions is shown in Table 4. Almost 80% and 65% of the BACs and WGP contigs of S or T origins were indicated to be linked to S or T linkage group regions, respectively.

Figure S1 shows, for each linkage group, the location of SSR markers of S or T origin used for the genetic map construction on the left and that of the BACs of S or T origins that are linked to the tobacco genetic map on the right. The linkage groups are colored according to their S or T annotation from Bindler et al. (Bindler, *et al.* 2011) For linkage group 22, a color inversion in the S and T assignment is visible in Figure 1 of Bindler et al. (Bindler, *et al.* 2011). Recalculation of ancestral origins after correcting this possible inversion increased the fraction of BACs for which the predicted origin corresponds with the genetic map and decreased discrepant cases by about 2% (Table S4).

Discussion

The WGP physical map of the tobacco genome was constructed from 51 nt WGP tags. Because the Illumina GA sequencing technology we employed produced longer sequence reads, additional maps using longer (70 nt) and shorter (31 nt) tags were also constructed to investigate the influence of tag length on map resolution. Although longer sequence reads may discern more unique WGP tags from the genome, sequence errors over longer read lengths may decrease the actual number of deconvoluted WGP tags following our criteria of requiring three observations per tag per dimension. Hence, we observed the largest number of deconvoluted reads at 51 nt tags and chose this tag length as reference for our WGP maps. However, we generated six WGP maps by combining different tag lengths (31, 51 and 70 nt)

and FPC stringency levels (“high” and “normal” stringency) and concluded that although small differences in the map metrics were observed, the six maps were highly similar. In general, the use of a higher stringency for physical map construction using FPC resulted in more WGP contigs, obtained in the vast majority of cases by the splitting of “normal” stringency WGP contigs at points where the BAC coverage is low. Major rearrangements of the BAC orders between the different maps were not observed.

Determination of the ancestral origin of WGP tags, BACs and WGP contigs showed that a higher proportion of elements were of S origin than of T origin, regardless of the category. The WGP physical map is expected to cover the whole tobacco genome, and therefore the WGP contigs and the underlying BACs and WGP tags are unlikely to be biased towards one of the two ancestors. The evolutionary distance of *N. sylvestris* and *N. tomentosiformis* from their respective ancestors involved in the hybridization event that gave rise to *N. tabacum* is unclear (Ren and Timko 2001, Moon *et al.* 2008). Assuming that after hybridization, both ancestral genomes evolved at the same rate in tobacco, the proportion of WGP tags of S or T origin would indicate that *N. sylvestris* is closer to the S ancestor than *N. tomentosiformis* is to the T ancestor. The relationship between *N. tabacum* and *N. sylvestris* is well established, whereas that between *N. tabacum* and *N. tomentosiformis* has been challenged regularly by a third *Nicotiana* species, *N. otophora* (Ren and Timko 2001, Murad *et al.* 2002). Extending the current work (tag sequencing based on genomic DNA) to the latter species might help to resolve this issue.

An initial conclusion that can be drawn from Table 2 is that one-third of the *N. tabacum* (Hicks Broadleaf) WGP tags are not present or are undetectable in *N. sylvestris* or *N. tomentosiformis*. At the BAC level, it was shown that the fraction of BACs for which no

origin could be determined was 1.5%. The presence of 0.4% of BACs with an undefined origin is not surprising and this small fraction is hypothesized to correspond largely to BACs covering regions where recombination between the S and T ancestral genomes occurred. At the physical map level, 0.5% of the contigs have an undefined origin. Although a portion of this fraction may indicate contigs that were constructed inappropriately, this is expected to happen because the average size of the region covered by a contig is larger than that covered by a BAC, and hence there are more chances that it covers a cross-over point.

Although not in full agreement, the ancestry annotation of the SSR markers used to construct the genetic map of tobacco (Bindler, *et al.* 2011) and the predicted origin of the BACs linked to these markers correspond to a large extent. This indicates that the tag-based approach we demonstrate it is appropriate to infer the ancestral origin of a BAC or WGP contig.

In addition to the tobacco WGP map presented here, WGP physical maps of two other Solanaceae crops, potato and tomato, have been constructed (de Boer, *et al.* 2011, Orozco López 2012). Table S5 summarizes the metrics for the three maps. To accommodate for its larger genome size, longer tags were used for tobacco than for tomato and potato. Because of the differences in genome sizes, it is better to compare these numbers relative to total genome coverage. In this case, the number of unique tags per Mb is similar, at 274.8, 286.6 and 275.0 for tomato, potato and tobacco respectively, whereas the number of tagged BACs is larger for tobacco (80.1) than for tomato (69.3) and potato (59.2). After construction of the physical maps, 2.2 contigs per Mb were obtained for tobacco, which is less than the 2.6 and 3.1 contigs obtained for tomato and potato respectively. Similarly, the number of singletons per Mb for tobacco (6.7) is less than that for tomato (14.1) and potato (7.7). The average and N_{50}

contig sizes, both in BACs and kbp, are also higher for the tobacco map than for the tomato and potato maps. Collectively, these metrics indicate that the WGP physical map of tobacco is of comparable, or even slightly superior, quality to that of the tomato and potato physical maps.

The sequence-based WGP contigs can be used to scaffold DNA sequences and, via a genetic map, to assign them to pseudo-chromosomes. At the same time, DNA sequences can help the scaffolding of WGP contigs. A schematic illustration of how WGP contigs can be used to scaffold DNA sequences by taking advantage of the sequenced WGP tags is shown in Figure 2 A. We applied this strategy to the SGN assembly of the publicly available TGI reads to confirm its feasibility and obtained 167 scaffolds of two contigs, 23 scaffolds of three contigs, nine scaffolds of four contigs, and one scaffold of five contigs. The SGN assembly has an average contig size of 1,275 bp, which is shorter than the estimated average distance between two WGP tags (~3 kb). Because two mapped WGP tags from different regions of one WGP contig are necessary to obtain orientation information of a sequence in a scaffold, a large fraction of the SGN assembly contigs are probably not useable because of their short size. The inability to order tags within a WGP contig region limits the efficiency of the scaffolding in two ways. First, it prevents an accurate estimation of the distance between the scaffolded contigs, giving an approximate range only. Second, it prohibits the scaffolding of contigs that are mapped to the same regions, effectively making scaffolding using WGP contigs a tool for long-range scaffold construction. As such, WGP in its current configuration is complementary to other DNA sequence scaffolding approaches that target shorter scaffolding distances, such as EST- and mate-pair library-based scaffolding. Adaptations of the WGP protocol, e.g. the use of other restriction enzymes that cut more frequently and thus increase the tag density, may modulate these features of WGP. The BAC coverage and its

variation along the WGP contig can be used to assess the confidence that two contigs should be scaffolded, where a low coverage indicates possible misassembly of the WGP contig.

Although perhaps of less direct interest, WGP contigs and/or singleton BACs themselves can be scaffolded using DNA sequences. Such a strategy is illustrated in Figure 2 B. Its use to scaffold contigs from the WGP physical map using contigs from the SGN assembly of the publicly available TGI reads resulted in 17 scaffolds of two WGP contigs. As mentioned previously, the SGN assembly has an average contig size of only 1,275 bp and, at 37,736 bp, its longest contig covers only about one-third of a BAC. Again, the abundance of small contigs reduces the possibilities of scaffolding. Nevertheless, the few scaffolds obtained are sufficient to demonstrate how DNA sequences can be used to scaffold WGP contigs. A high-quality scaffolding will, of course, require longer DNA sequences and more stringent criteria to avoid erroneous scaffolding. Using multiple tags from different bins for each scaffolded WGP contig would be a first step in that direction.

A high-quality physical map of tobacco was constructed using WGP with metrics equivalent to those of tomato and potato. Benefiting from the fact that this map is based on sequenced DNA tags, and despite the lack of a full genome sequence, the ancestral origin of the BACs used in the physical map and the obtained WGP contigs was determined in 98% and 99% of the cases, respectively. When linked to the tobacco genetic map, this ancestry assignment was found to be in agreement with the results obtained with SSR markers. As is the case for other plants, the tobacco physical map can be used for DNA sequence scaffolding and will thus be of use in *de novo* sequencing and assembly of the tobacco genome. The combination of WGP map construction and tag sequencing of (putative) ancestral lines may

Accepted Article
be beneficial to unravel ancestry relationship in other polyploid organisms and does not require prior sequence information to obtain high-resolution ancestry information.

Agricultural crops grown in the field are frequently prone to abiotic (Tester and Bacic 2005, Vinocur and Altman 2005, Mittler 2006, Vij and Tyagi 2007) and biotic (Peterson and Higley 2000, Tolmay 2001, Cattivelli *et al.* 2008, Reynolds and Tuberosa 2008) stresses, which affect the yield, quality, harvesting time and other valuable characteristics. Genes conferring resistance to these stresses found in related wild plant species can be transferred to cultivars by utilizing numerous molecular biology methods. The physical mapping of such genes in naturally occurring *Nicotiana* species with the help of the tobacco physical map will facilitate plant biotechnology applications aimed at accelerating and increasing the precision of plant breeding for abiotic and biotic stress resistance.

Experimental procedures

BAC Libraries. Four BAC libraries of the allotetraploid genome of *N. tabacum* cv. Hicks Broadleaf (inbred line PI 552397 or TC 311 in the USDA-ARS-GRIN database), comprising a total of 425,088 BAC clones (1,107 384-well plates) and approximately 10.4× genome coverage, were used for construction of the WGP map. These libraries were (1) a *Hind*III library (Microsynth) consisting of 112,896 clones with an estimated average insert size of 100 kb, representing approximately 2.5× genome coverage; (2) a *Bam*HI library (Microsynth), consisting of 146,304 clones with an estimated average insert size of 100 kb, representing approximately 3.4× genome coverage; (3) an *Eco*RI library (PMTBE) consisting of 69,120 clones, with an estimated average insert size of 125 kb, representing approximately 1.9× genome coverage; and (4) a *Hind*III library (PMTBH), consisting of 96,768 clones with an estimated average insert size of 125 kb, representing approximately 2.7× genome coverage.

BAC library pooling, DNA isolation and WGP sample preparation. Individual BACs of the four libraries stored in 384-well plates were pooled in a two-dimensional (2D) format prior to DNA isolation. Specifically, BACs were 2D pooled by taking six plates at a time in a 2 × 3 layout (termed a SuperPool; SP) and pooling each row over two plates (48 BACs) and each column over three plates (48 BACs), yielding 96 pools per SP. BAC pools were subjected to isolation of high-concentration DNA and WGP sample preparation was performed essentially as described in (van Oeveren, *et al.* 2011). Briefly, AFLP[®] templates (Vos *et al.* 1995) were prepared from pooled BAC DNA by digestion using 5 U *EcoRI* and 2 U *MseI*. Next, adapter ligation was carried out using either a P5 *EcoRI* adaptor containing a 5 or 6 nt sample identification tag in combination with a unique P7 *MseI* adaptor (when one or two SPs were pooled per lane for sequencing), or using a P5 *EcoRI* adaptor containing a 5 nt sample identification tag and P7 *MseI* adaptor with a 3 nt sample identification tag (when three SPs were pooled for sequencing in one lane). PCR was performed in 20 µl volumes and contained 5 µl 10-fold diluted restriction ligation mixture, 30 ng Illumina P5 primer (5'-AATGATACGGCGACCACCG-3'), 30 ng Illumina P7 primer (5'-CAAGCAGAAGACGGCATAACGA-3'), 0.2 mM dNTPs, 0.4 U Amplitaq (Applied Biosystems) and 1× Amplitaq buffer. Next, equal amounts of BAC pool PCR reaction mixtures were pooled per SP and purified using the QIAquick PCR Purification Kit (Qiagen). In case one or two SPs were sequenced per lane, each BAC pool was barcoded by one of 192 different 5 or 6 nt sample identification tags in the P5 *EcoRI* adapter. In case three different SPs were combined for sequencing in one lane, each BAC pool was tagged by a combination of one of 96 different P5 *EcoRI* adapters with a 5 nt sample identification tag and one of three different P7 *MseI* adapters with a 3 nt sample identification tag, such that 288 BAC pools could be pooled per lane for sequencing.

Sequencing. A total of 90 lanes of either 76 or 78 cycles of sequencing, divided over 15 runs, were performed using an Illumina Genome Analyzer II. Sequencing with 76 cycles was employed in case one or two SPs were pooled per lane, whereas 78-cycle sequencing with a second priming event at the *MseI* side was used when three SPs were pooled per lane, in which case the 3 nt sample identification tags at the *MseI* side were determined. Each run used a flow cell with eight lanes of physically separated samples, such that the same set of sample tags were used for each lane. *GAI* runs were performed comprising seven lanes with tobacco WGP samples at 5.5 pM concentration, each covering one, two or three SPs represented in 96, 192 or 288 row and column pools, respectively. The Illumina pipeline software was used to extract sequence reads of 76 or 78 nt length from the images. An additional quality filter was applied to select only those reads with all base calls having at least a Solexa quality of 0 (equivalent to a Phred quality of 3) on the Illumina GA scale. All sequence data have been deposited in the European Nucleotide Archive (ENA) under accession number ERP001765.

Deconvolution and filtering. Sequence reads were split into three parts in the case of 76-cycle sequencing or in four parts in the case of 78-cycle sequencing to enable assignment of unique tags to pools and to allow for consecutive deconvolution into individual BACs. In the case of 76-cycle sequencing the first 5 (or 6) nt represented the sample (i.e. BAC pool) identification tag at the *EcoRI* side; the next 6 nt matched the *EcoRI* restriction site of the adapter and the remaining nucleotides defined the “WGP tag”. In the case of 78-cycle sequencing with combinatorial barcoding at the *EcoRI* and *MseI* side ends, a fourth part representing the 3 nt sample identification tag at the *MseI* side was obtained.

Three different WGP tag lengths were analyzed to test the effect of read length on WGP map resolution: 31 nt, 51 nt and 70 nt (all including the *EcoRI* restriction site). The

assignment of unique WGP tags to individual BACs was based on the following criteria: 1) A specific WGP tag must occur in two pools to indicate its unique position on the plate - one column and one row pool with both being represented by at least three reads; and 2) if WGP tags are inadvertently observed in a third or fourth pool, the number of reads in these other pools must be less than a tenth of those in the smallest true pool. WGP tags not matching these criteria were discarded. A script was used to recognize and trim the sample identification tags, the restriction site part of the sequence reads and to perform the deconvolution. Unique WGP tags were defined by grouping them in 100% identical read sets. The output of this procedure consisted of a list of all WGP tags, the corresponding number of reads, and the identification number of the BAC they were assigned to. Finally, a filtering step was applied to remove the WGP tags matching vector, *Escherichia coli* or chloroplast sequences, containing homopolymer sequences of 5 nt or longer, and WGP tags occurring on just a single BAC.

Contig building. Contigging was performed using the FPC program (Soderlund, *et al.* 1997). This software tool was originally developed for analyzing BAC fingerprint data: restriction fragments determined by their length. The WGP tags were adapted for use in FPC as described in (van Oeveren, *et al.* 2011) by converting them into numbers to yield pseudo restriction fragment sizes for which the software was originally designed. As the WGP tags are uniquely defined by their sequence composition, FPC could be used at the highest stringency setting of tolerance (value = 0). Different cut-off values were tested, specifying the threshold on the probability of BAC coincidence, i.e. the likelihood that different BACs containing partly overlapping sets of WGP tags originate from the same genomic region. The output of FPC consisted of a list with contigs and the corresponding order of BACs within each contig. The genome coverage, average contig size and N₅₀ contig size in million base

pairs were estimated by multiplying FPC band units by the average distance between two WGP tags. The latter was estimated by dividing the average BAC insert size by the average number of WGP tags.

Linking of BACs to the genetic map. To identify BACs containing SSR markers, 1,185 SSR primer pairs were screened from pools and superpools of 196 *Bam*HI and 193 *Hind*III BAC library plates representing about 3× coverage (~149,000 BACs) of the tobacco genome.

Determination of Ancestral origin. Nuclear genomic DNA was isolated from seedling leaf material of *N. sylvestris* TW138 and *N. tomentosiformis* TW142 (USNGC) in accordance with a protocol for HMW nuclear DNA extraction (Liu and Whittier 1994). As the *N. tomentosiformis* line did not yield enough nuclear DNA, genomic DNA isolation was performed using the Nucleon Plant Genomic DNA Extraction Kit (Gen-probe) according to the manufacturer's specifications to obtain ample material. DNA samples were used for *Eco*RI/*Mse*I (E/M) AFLP template preparation as described in (Vos, *et al.* 1995), using two different barcoded adaptors suitable for *GAI*I sequencing, in a similar approach to the WGP sample preparation. Seven lanes of a single *GAI*I run were used with a read length of 75 nt, yielding 63.9 million reads for these two samples. Reads for which one or more sequenced nucleotide had a quality lower than 20 (i.e., a probability of error of 0.01) were discarded. For both ancestral species, unique sequences of length 51 nt were grouped into tags, and tags found in both species or with only one read were removed.

The S or T ancestral origin of each BAC included in the physical map construction and each WGP contig was determined by calculating the S or T enrichment *P*-values. The proportion of S-tags (respectively T-tags), weighted according to its number of reads in *N.*

sylvestris (respectively *N. tomentosiformis*), was computed for each BAC or WGP contig. If the BAC or WGP contig was enriched by S-tags (respectively T-tags), the estimated proportion was far from a random selection of tags from the original pool. Therefore, an enrichment *P*-value for S-tags and T-tags proportion was estimated using the hypergeometric distribution for the null hypothesis. The obtained *P*-values were subsequently corrected for multiple testing effects using the Benjamini-Hochberg false discovery rate (Benjamini and Hochberg 1995). The ancestral origin of a BAC or WGP contig was predicted to be S (respectively T) if the enrichment *P*-value for S (respectively T) was less than 10^{-6} and the enrichment *P*-value for T (respectively S) was above 10^{-6} , otherwise the origin was undefined.

To elucidate the ancestral structure of a WGP contig, each WGP contig unit, as defined by the FPC software, was assigned a putative label S (respectively T) if the number of S (respectively T) BACs covering the unit exceeds the 95% quantile of a binomial distribution of parameter 0.5. Otherwise the unit was labeled “undefined”. The advantage of using this quantile over a constant threshold is to penalize sparser regions of the WGP contig. Once putative labels were assigned, the WGP contig was split into connected S (respectively T, undefined) segments by mimicking a classification and regression tree approach (see e.g. (Hastie *et al.* 2001)). To control the level of smoothing a minimum segment size of 40 was chosen. The binary rules obtained were then parsed to extract the structure of the WGP contig. Each segment of a given origin was called a domain of the WGP contig.

Scaffolding. The position on a WGP contig covered by all the BACs containing a given WGP tag, and by no other BACs, was calculated for all WGP tags belonging to only one WGP contig. These WGP tags were mapped to the Sol Genomics Network version 1

assembly of the Tobacco Genome Initiative (TGI) reads, and perfect matches were kept. Assembly contigs with at least two mapped WGP tags from two different parts of the same WGP contig were selected, as they could be mapped with orientation to the WGP contig. Non-overlapping assembly contigs mapping to the same WGP contig were scaffolded. Assembly contigs with mapped WGP tags from two different WGP contigs were used to scaffold these WGP contigs. The position of the WGP tags and of the BACs in the 51nt normal stringency WGP physical map are shown in Table S6 and Table S7, respectively.

Acknowledgement

The authors thank Gregor Bindler for providing seeds for *N. tabacum*, *N. sylvestris* and *N. tomentosiformis*, and Microsynth AG for identification of BACs containing SSR markers. The authors are grateful to Nicolas Bakaher and Lucien Bovet for their critical comments on the manuscript. The AFLP[®] and WGP[™] technologies are covered by patents and patent applications owned by Keygene N.V. AFLP, WGP and KeyGene are (registered) trademarks of Keygene N.V. Other trademarks are the property of their respective owners. Research described in this article was supported by Philip Morris International.

Supporting information figure legends

Figure S1. SSR (left) and BAC (right) markers of S or T origin used for the genetic map construction. Linkage groups are colored according to their S or T annotation from Bindler et al. (6)

Table S1. Number of BACs and WGP tags for the physical map construction using 31, 51 or 70 nt tags

Table S2. Metrics of the normal and high stringency physical maps constructed with 31, 51 or 70 nt tags

Table S3. Distribution of domains of S or T genome origin counted in WGP contigs of S, T or undefined origin. The maximum number of domains is six, composed of undefined and a single ancestor (S or T)

This article is protected by copyright. All rights reserved.

Table S4. Comparison of determined ancestral origins of BACs and WGP contigs to the putative origin assigned to linkage group regions following correction for the inversion of the S and T annotation of linkage group 22

Table S5. Metrics for the WGP physical maps of tomato, potato and tobacco

Table S6. Positions of the BAC in the 51nt normal stringency WGP physical map of the tobacco genome. Columns are the BAC number, the WGP contig, the start position in the WGP contig, and the end position in the WGP contig.

Table S7. Position and ancestral origin of WGP tag in the 51nt normal stringency WGP physical map of the tobacco genome. Columns are the WGP tag number, the ancestral origin of the WGP tag, the WGP contig, the start position in the WGP contig, and the end position in the WGP contig.

References

- Ariyadasa, R. and Stein, N.** (2012) Advances in BAC-Based Physical Mapping and Map Integration Strategies in Plants. *Journal of Biomedicine and Biotechnology*, **184854**, 1-11.
- Arumuganathan, K., Martin, G.B., Telenius, H., Tanksley, S.D. and Earle, E.D.** (1994) Chromosome 2-specific DNA clones from flow-sorted chromosomes of tomato. *Mol Gen Genet*, **242**, 551-558.
- Benjamini, Y. and Hochberg, Y.** (1995) Controlling the False Discovery Rate: A Practical and Powerful Approach to Multiple Testing. *Journal of the Royal Statistical Society. Series B (Methodological)*, **57**, 289-300.
- Bindler, G., Plieske, J., Bakaher, N., Gunduz, I., Ivanov, N., Van der Hoeven, R., Ganal, M. and Donini, P.** (2011) A high density genetic map of tobacco (*Nicotiana tabacum* L.) obtained from large scale microsatellite marker development. *Theor Appl Genet*, **123**, 219-230.

- Bombarely, A., Menda, N., Teclé, I.Y., Buels, R.M., Strickler, S., Fischer-York, T., Pujar, A., Leto, J., Gosselin, J. and Mueller, L.A.** (2011) The Sol Genomics Network (solgenomics.net): growing tomatoes using Perl. *Nucleic Acids Res*, **39**, D1149-1155.
- Cattivelli, L., Rizza, F., Badeck, F.W., Mazzucotelli, E., Mastrangelo, A.M., Francia, E., Mare, C., Tondelli, A. and Stanca, A.M.** (2008) Drought tolerance improvement in crop plants: An integrated view from breeding to genomics. *Field Crops Research*, **105**, 1-14.
- Clarkson, J.J., Lim, K.Y., Kovarik, A., Chase, M.W., Knapp, S. and Leitch, A.R.** (2005) Long-term genome diploidization in allopolyploid *Nicotiana* section *Repandae* (Solanaceae). *New Phytol*, **168**, 241-252.
- de Boer, J.M., Borm, T.J.A., Jesse, T., Brugmans, B., Tang, X., Bryan, G.J., Bakker, J., van Eck, H.J. and Visser, R.G.F.** (2011) A hybrid BAC physical map of potato: a framework for sequencing a heterozygous genome. *BMC genomics*, **12**, 594.
- Ding, Y., Johnson, M., Chen, W., Wong, D., Chen, Y., Benson, S., Lam, J., Kim, Y. and Shizuya, H.** (2001) Five-color-based high-information-content fingerprinting of bacterial artificial chromosome clones using type IIS restriction endonucleases. *Genomics*, **74**, 142-154.
- Hastie, T., Tibshirani, R. and Friedman, J.H.** (2001) *The elements of statistical learning: Data mining, inference, and prediction*. New York: Springer Verlag.
- Leitch, I.J., Hanson, L., Lim, K.Y., Kovarik, A., Chase, M.W., Clarkson, J.J. and Leitch, A.R.** (2008) The ups and downs of genome size evolution in polyploid species of *Nicotiana* (Solanaceae). *Ann Bot*, **101**, 805-814.
- Lim, K.Y., Skalicka, K., Koukalova, B., Volkov, R.A., Matyasek, R., Hemleben, V., Leitch, A.R. and Kovarik, A.** (2004) Dynamic changes in the distribution of a

satellite homologous to intergenic 26-18S rDNA spacer in the evolution of *Nicotiana*. *Genetics*, **166**, 1935-1946.

Lin, L., Pierce, G.J., Bowers, J.E., Estill, J.C., Compton, R.O., Rainville, L.K., Kim, C., Lemke, C., Rong, J. and Tang, H. (2010) A draft physical map of a D-genome cotton species (*Gossypium raimondii*). *BMC genomics*, **11**, 395.

Liu, Y.G. and Whittier, R.F. (1994) Rapid preparation of megabase plant DNA from nuclei in agarose plugs and microbeads. *Nucleic Acids Res*, **22**, 2168-2169.

Luo, M.C., Thomas, C., You, F.M., Hsiao, J., Ouyang, S., Buell, C.R., Malandro, M., McGuire, P.E., Anderson, O.D. and Dvorak, J. (2003) High-throughput fingerprinting of bacterial artificial chromosomes using the snapshot labeling kit and sizing of restriction fragments by capillary electrophoresis. *Genomics*, **82**, 378-389.

Luo, M.C., Ma, Y., You, F.M., Anderson, O.D., Kopecký, D., Šimková, H., Šafář, J., Doležel, J., Gill, B. and McGuire, P.E. (2010) Feasibility of physical map construction from fingerprinted bacterial artificial chromosome libraries of polyploid plant species. *BMC genomics*, **11**, 122.

Mittler, R. (2006) Abiotic stress, the field environment and stress combination. *Trends in plant science*, **11**, 15-19.

Moon, H.S., Nicholson, J.S. and Lewis, R.S. (2008) Use of transferable *Nicotiana tabacum* L. microsatellite markers for investigating genetic diversity in the genus *Nicotiana*. *Genome*, **51**, 547-559.

Murad, L., Lim, K.Y., Christopodulou, V., Matyasek, R., Lichtenstein, C.P., Kovarik, A. and Leitch, A.R. (2002) The origin of tobacco's T genome is traced to a particular lineage within *Nicotiana tomentosiformis* (Solanaceae). *Am J Bot*, **89**, 921-928.

Orozco López, M. (2012) The tomato genome sequence provides insights into fleshy fruit evolution. *Nature*, 2012, vol. 485, p. 635-641.

- Peterson, R.K.D. and Higley, L.G.** (2000) *Biotic stress and yield loss*: CRC.
- Rabinowicz, P.D., Schutz, K., Dedhia, N., Yordan, C., Parnell, L.D., Stein, L., McCombie, W.R. and Martienssen, R.A.** (1999) Differential methylation of genes and retrotransposons facilitates shotgun sequencing of the maize genome. *Nat Genet*, **23**, 305-308.
- Ren, N. and Timko, M.P.** (2001) AFLP analysis of genetic polymorphism and evolutionary relationships among cultivated and wild *Nicotiana* species. *Genome*, **44**, 559-571.
- Reynolds, M. and Tuberosa, R.** (2008) Translational research impacting on crop productivity in drought-prone environments. *Current opinion in plant biology*, **11**, 171-179.
- Soderlund, C., Longden, I. and Mott, R.** (1997) FPC: a system for building contigs from restriction fingerprinted clones. *Comput Appl Biosci*, **13**, 523-535.
- Tester, M. and Bacic, A.** (2005) Abiotic stress tolerance in grasses. From model plants to crop plants. *Plant Physiology*, **137**, 791-793.
- Tolmay, V.L.** (2001) Resistance to biotic and abiotic stress in the Triticeae. *Hereditas*, **135**, 239-242.
- van Oeveren, J., de Ruiter, M., Jesse, T., van der Poel, H., Tang, J., Yalcin, F., Janssen, A., Volpin, H., Stormo, K.E., Bogden, R., van Eijk, M.J. and Prins, M.** (2011) Sequence-based physical mapping of complex genomes by whole genome profiling. *Genome Res*, **21**, 618-625.
- Vij, S. and Tyagi, A.K.** (2007) Emerging trends in the functional genomics of the abiotic stress response in crop plants. *Plant Biotechnology Journal*, **5**, 361-380.
- Vinocur, B. and Altman, A.** (2005) Recent advances in engineering plant tolerance to abiotic stress: achievements and limitations. *Current Opinion in Biotechnology*, **16**, 123-132.

Vos, P., Hogers, R., Bleeker, M., Reijans, M., van de Lee, T., Hornes, M., Frijters, A.,

Pot, J., Peleman, J., Kuiper, M. and et al. (1995) AFLP: a new technique for DNA fingerprinting. *Nucleic Acids Res*, **23**, 4407-4414.

Wei, F., Zhang, J., Zhou, S., He, R., Schaeffer, M., Collura, K., Kudrna, D., Faga, B.P.,

Wissotski, M. and Golser, W. (2009) The physical and genetic framework of the maize B73 genome. *PLoS Genetics*, **5**, e1000715.

Xu, X., Pan, S., Cheng, S., Zhang, B., Mu, D., Ni, P., Zhang, G., Yang, S., Li, R. and

Wang, J. (2011) Genome sequence and analysis of the tuber crop potato. *Nature*, **475**, 189.

Zhang, M., Zhang, Y., Huang, J.J., Zhang, X., Lee, M.K., Stelly, D.M. and Zhang, H.B.

(2012) Genome Physical Mapping of Polyploids: A BIBAC Physical Map of Cultivated Tetraploid Cotton, *Gossypium hirsutum* L. *PloS one*, **7**, e33644.

Tables

Table 1. Metrics for the physical map construction using a 51 nt tag length

Number of BACs tested	425,088
Genome equivalents	10.4
Number of deconvolutable reads (M)	907.7
Number of unique WGP tags	1,239,733
Number of tagged BACs (FPC ready)	361,034
% tagged BACs (FPC ready)	85%
Average number of tags/BAC	32.1
Number of contigs	9,750
Number of BACs in contigs	330,632
Number of singletons	30,402
Average # BACs/contig	34
N50 BACs/contig	60
Average contig size (Mbp)	0.462
N50 contig size (Mbp)	0.689
Genome coverage (Mbp)	4,508
% genome coverage	100%

Table 2. Ancestral origin of the WGP tags, BACs and contigs

	S origin	T origin	Undefined origin	Unknown origin
WGP tags	494,973 (39.9%)	311,399 (25.1%)	0 (0.0%)	433,361 (35.0%)
BACs	219,143 (60.7%)	134,933 (37.4%)	1,375 (0.4%)	5,583 (1.5%)
WGP contigs	5,236 (53.7%)	4,465 (45.8%)	45 (0.5%)	4 (0.0%)

Table 3. Number and proportion of BACs classified to their ancestral origin compared to the ancestral origin of the WGP contigs to which they belong

BAC	WGP contig			
	S origin	T origin	Undefined origin	Unknown origin
S origin	199,254 (98.0%)	3,155 (1.6%)	861 (0.4%)	0 (0.0%)
T origin	6,647 (5.3%)	117,989 (94.0%)	833 (0.7%)	0 (0.0%)
Undefined origin	491 (43.8%)	595 (53.1%)	35 (3.1%)	0 (0.0%)
Unknown origin	150 (19.4%)	603 (78.1%)	10 (1.3%)	9 (1.2%)

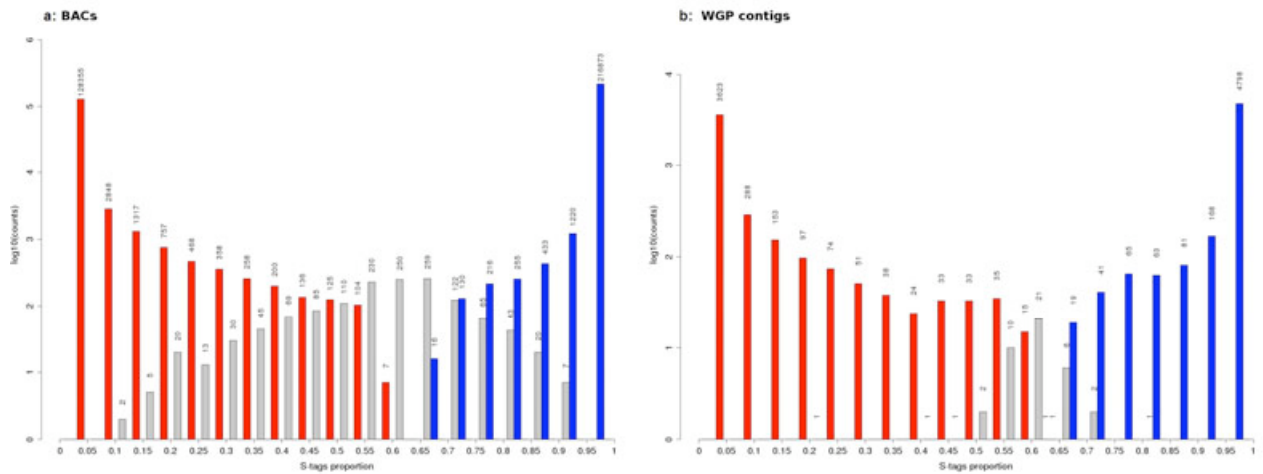
Table 4. Comparison of determined ancestral origins of BACs and WGP contigs to the putative origin assigned to linkage group regions

	S origin	T origin	Undefined origin	Unknown origin
S linkage group regions				
BACs	331 (78.8%)	88 (21.0%)	1 (0.2%)	0 (0.0%)
WGP contigs	308 (79.0%)	81 (20.8%)	1 (0.3%)	0 (0.0%)
T linkage group regions				
BACs	118 (30.7%)	262 (68.2%)	3 (0.8%)	1 (0.3%)
WGP contigs	128 (35.8%)	227 (63.4%)	3 (0.8%)	0 (0.0%)

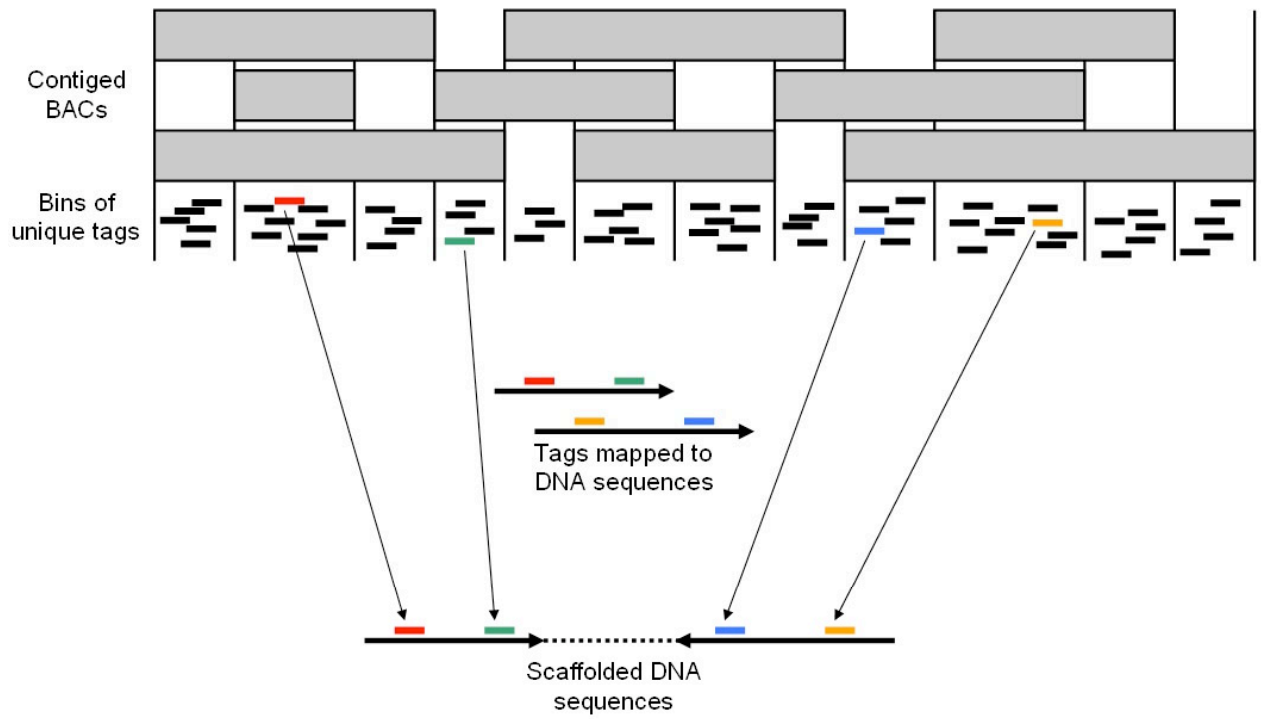
Figure legends

Figure 1. Log-10 frequency of the weighted proportion of S tags. A value of 0 indicates a T origin (red bars) and a value of 1 an S origin (blue bars), according to the enrichment *P*-values (see Materials and Methods section). The grey bars indicate counts of (A) BACs or (B) WGP contigs of undefined origin, i.e. for which unequivocal assignment to S or T was not possible. Absolute counts are given above each bar.

Figure 2. Strategies to scaffold DNA sequences using the WGP physical map and scaffold WGP contigs using DNA sequences. (A) Scaffolding of DNA sequences using the WGP physical map. The orientation of the scaffolded DNA sequences is indicated by the mapping position of WGP tags from different bins of the same WGP contigs. (B) Scaffolding of WGP contigs using DNA sequences. Tags from end bins of different WGP contigs mapping to the same DNA sequence are used to link WGP contigs.



a: Scaffolding of DNA sequences



b: Scaffolding of WGP contigs

